processes

MDPI

Article

Removal of Paracetamol and Cu^{2+} from Water by Using Porous Carbons Derived from Agrowastes

Regiane C. Ferreira [1], Thiago Peixoto de Araújo [2], Diogo Dias [3], Maria Bernardo [3,*], Nuno Lapa [3,*], Isabel M. Fonseca [3] and Maria A. S. D. de Barros [4]

[1] Departamento EAD de Engenharia Híbridos, Centro Universitário de Maringá—UNICESUMAR, Av. Guedner, 1610—Jardim Aclimação, Maringá 87050-900, Paraná, Brazil; regiane.cristina.1989@gmail.com
[2] Departamento de Engenharia Química, Universidade Tecnológica Federal do Paraná—Campus Ponta Grosa, Ponta Grossa 84017-220, Paraná, Brazil; thiago@flashrg.com.br
[3] LAQV/REQUIMTE, Department of Chemistry, NOVA School of Science and Technology, NOVA University Lisbon, 2829-516 Caparica, Portugal; da.dias@campus.fct.unl.pt (D.D.); blo@fct.unl.pt (I.M.F.)
[4] Departamento de Engenharia Química, Universidade Estadual de Maringá, Av. Colombo 5790, Maringá 87020-900, Paraná, Brazil; angelicabarros.deq@gmail.com
* Correspondence: maria.b@fct.unl.pt (M.B.); ncsn@fct.unl.pt (N.L.)

Abstract: Dende and babassu coconuts are largely used in tropical countries, namely in Brazil, for the extraction of oils from kernels. The remaining biowastes are industrially processed to produce porous carbons (PCs). PCs derived from dende and babassu biowastes and produced at an industrial scale have been characterized by textural, chemical, and ecotoxicological parameters. A commercial activated carbon (CC) of mineral origin has been used as a benchmarking material. Although the CC sample presented a higher surface area (S_{BET} = 1083 m^2/g), the PCs derived from the biowastes were richer in micropores (V_{micro} = 0.25–0.26 cm^3/g), while the CC carbon presented wider pore size distribution with a higher mesopore volume (V_{meso} = 0.41 cm^3/g). All the adsorbents used in this work have shown a non-acute ecotoxic behavior for the bacterium *Vibrio fischeri* (EC_{50}-30 min > 99% *v/v*). The adsorbents have been tested for paracetamol and Cu^{2+} adsorption in mono- and bicomponent solutions. The uptake capacities of paracetamol (q_e, 98–123 mg g^{-1}) and Cu^{2+} (q_e, 15–18 mg g^{-1}) from monocomponent solutions were similar to the ones obtained in the bicomponent solutions, indicating no competition or cooperative effects but a site-specific adsorption. This finding represents an advantage for the removal of these adsorbates when present in the same solution as they can be adsorbed under similar rates as in the single systems. Paracetamol adsorption was related to micropore filling, π-π interactions, and H-bonding, whereas Cu^{2+} removal was attributed to the cation exchange mechanism and complexation to the hydroxyl groups at the carbons' surface.

Keywords: biowastes; activated porous carbons; adsorption; single system; binary system

Citation: Ferreira, R.C.; de Araújo, T.P.; Dias, D.; Bernardo, M.; Lapa, N.; Fonseca, I.M.; de Barros, M.A.S.D. Removal of Paracetamol and Cu^{2+} from Water by Using Porous Carbons Derived from Agrowastes. *Processes* **2023**, *11*, 2146. https://doi.org/10.3390/pr11072146

Academic Editors: Isabel Cansado, Silvia Roman Suero, Paulo Alexandre Mira Mourão, Suhas, José Castanheiro and David W. Mazyck

Received: 24 May 2023
Revised: 12 July 2023
Accepted: 15 July 2023
Published: 18 July 2023

1. Introduction

In Brazil, babassu production in 2021 reached 32,074 tons of kernels, being an important economic activity for rural traditional communities. Babassu is present mainly in the states of Piauí, Tocantins, and Mato Grosso, and in greater quantities in the state of Maranhão, which in 2021 concentrated 90% of almond extraction [1]. The babassu coconut has a fibrous layer called epicarp. This fiber constitutes 12.6% of the fruit weight and involves an essential layer, the mesocarp or pulp, which is rich in starch and fiber. The mesocarp has 20.4% weight of the babassu fruit. Immediately further inside is the endocarp, which is responsible for 58.4% weight of the raw fruit. It is a very resistant layer around 2 to 3 cm thick, which is essential for the production of charcoal. Finally, at the core of the fruit are the kernels, which correspond to 8.7% of the babassu fruit weight. The babassu oil is extracted from these kernels [2].

Like babassu, dende oil or palm oil is widely used in Brazil. In 2022, the world palm oil production is estimated to reach 79,564 × 10^3 Mt [3]. The ranking is led by Indonesia, with a production of 47,000 × 10^3 Mt, followed by Malaysia with a production of 19,300 × 10^3 Mt. Brazil is in 10th place with a production of 585 × 10^3 Mt. Within Brazil, the Pará state represents 84% of the total dende oil production while Bahia state represents 16%.

Several biowastes are generated during the processing of dende and babassu coconuts, such as the outer layer of the epicarp, endocarp, and kernel cake resulting from the oil extraction. There are already several valorization pathways for these biowastes such as the production of fibers from the epicarp, flour from the mesocarp, charcoal from the endocarp, and biofuels, among others [2,4,5].

Some industries have envisaged other noble valorization pathways for babassu and dende coconut biowastes such as their conversion into porous carbons for which several adsorption applications have been studied [6–10].

The use of activated carbons to remove pharmaceutically active compounds (PhACs) from aqueous solutions has been largely studied, particularly those derived from agro-industrial biowastes, such as babassu and dende coconut [7,11], almond shell [12], paper mill sludge [13], dende (palm) kernel shell [14], among other biowastes as indicated in some review papers [15–17].

Conventional water and wastewater treatment plants are unable to completely remove micro-pollutants such as PhACs; therefore, these compounds can reach natural ecosystems through the discharge of treated wastewaters [18]. Generally, PhACs and their metabolites are excreted through the urine and feces being currently found in raw wastewaters, treated wastewaters, and sewage sludge. Also, hospital effluents and livestock are responsible for the presence of these compounds in the environment [19,20]. Despite the evidenced toxicity to aquatic organisms [21], caffeine, salicylic acid, carbamazepine, and acetaminophen, among other compounds, have been detected in treated wastewaters, which demonstrates the inefficiency of conventional primary, secondary, and tertiary treatment systems existing in the wastewater treatment plants concerning the removal of PhACs [19,22].

The non-prescribed analgesic acetaminophen, commercially known as paracetamol, is already considered one of the six most frequent pharmaceutical compounds present in water bodies and drinking water [19,22–24] with proven ecological risks [25,26].

Besides PhACs, ions of heavy metals, such as Cu^{2+}, are also commonly found in water bodies [27–29]. Copper has been known for many decades as a pollutant for aquatic ecosystems, not only concerning the water itself but also the sediments and biota. Although copper is an essential element for the metabolism in humans and animals, under certain concentrations and physicochemical conditions, it can pose risks to the environment, human health, and animals [30–32]. According to Luo et al. [33], copper is a chalcophile element that is widely spread in the earth's mantle and crust. Therefore, it must be assumed that this is a ubiquitous element in natural ecosystems. However, depending on the environmental conditions, it must be present in different oxidation states, which affects its solubility in water and mobility through the environment. In natural ecosystems without the influence of anthropogenic activities, their concentrations are usually low. Higher and toxic concentrations in soil and aquatic ecosystems are due to the discharge of liquid and solid wastes from industrial activities into the environment [34]. In this context, copper must be present in industrial effluents together with other organic and inorganic contaminants.

Adsorption processes are typically easy, simple, and cost-effective engineering solutions, and can improve substantially the treatment of wastewaters. Highly efficient adsorbents obtained from low-cost and renewable raw materials have been studied with notable efficiency in micropollutants' removal [16,35]. The conversion of biowastes into high-value porous carbons for the removal of contaminants has several advantages, such as the low cost of precursors and the valorization of wastes that frequently are discarded.

In the present work, babassu and dende biowastes have been used as precursors of porous activated carbons at an industrial plant. The authors have previously demonstrated

the high potential of babassu and dende-derived activated carbons for paracetamol removal in a single system [6,11]. However, the simultaneous removal of paracetamol with metals has been poorly investigated. This is a relevant topic as water-soluble complexes of heavy metals and pharmaceutical compounds can be formed in aqueous solutions when occurring simultaneously, presenting challenges to their removal. Although some studies have been dedicated to the simultaneous removal of PhACs and heavy metals (Cu, Ni, Pb, Cd) [36], most of those studies only consider PhACs from the antibiotic class, neglecting the coexistence of other pharmaceutical classes with heavy metals. Cu ions are amongst the most frequent heavy metals present in surface and groundwaters and although its toxicity is lower when compared to other heavy metals such as Pb, Cr, or Cd, it was previously observed that Cu ions are able to interact with PhACs generating complexes of higher toxicity [36] being more difficult to remove.

Recently, Ferreira et al. (2022) [37] have studied the simultaneous removal of paracetamol with Cu^{2+} ions by using bone char, and a cooperative adsorption mechanism was observed. The present work intends to give continuity to that study by evaluating the competitiveness/cooperativeness between both adsorbates when removed with low-cost carbons from babassu and dende biowastes. The performance of the biomass-derived carbons was compared with a commercial activated carbon.

2. Materials and Methods

2.1. Origin of Carbon Materials

The carbons derived from babassu coconut biomass (BBS) were produced by Tobasa Bioindustrial de Babaçu S.A. (Tocantins, Brazil). The carbons derived from dende coconut (DND) were produced by Bahiacarbon Agro Ind. (Bahia, Brazil). Due to industrial property rights, the production processes cannot be disclosed in this work. A commercial activated carbon (NORIT GAC 1240W) (NOR) was used as a benchmark. All carbons were sieved for a particle size of 0.210–0.250 mm. The supplied carbons were previously washed with deionized water until the pH of the washing water become stable. Afterwards, the washed carbons were oven-dried at 60 °C for 24 h and stored until their use.

2.2. Characterization of Carbon Materials

The proximate analysis was determined by the gravimetric method: moisture content (M) was determined at 105 °C (EN 14774-1:2009), volatile matter (VM) at 900 °C (EN 15148:2009), and ashes (Ash) at 750 °C (ASTM D1762). The fixed carbon (FC) was calculated by the difference: FC = 100 − (M + VM + Ash).

The elemental analysis (C, H, N, and S content) was carried out using a Thermo Finnigan elemental analyzer (CE Instruments, model Flash EA 1112 CHNS series).

Thermogravimetric analysis (TGA) was performed between 30 °C and 850 °C, by using a heating rate of 5 °C min^{-1}, under a continuous argon flow (Setaram Lab-sys EVO).

The pH at the point of zero-charge (pHpzc) was established by using pH shift analysis, according to the following procedure: 0.1 mol L^{-1} NaCl solutions with initial pH values between 2.0 and 12.0 were prepared (pH adjustment was performed with solutions of NaOH or HCl 0.01–1 mol L^{-1}). A mass of 0.1 g of the activated carbons was added to 20 mL of each NaCl 0.1 mol L^{-1} solution. The mixtures were stirred for 24 h and the final pH was measured. The pHpzc value corresponds to the plateau of the pH_{final} vs. $pH_{initial}$ curve.

The bulk mineral content was determined by microwave-assisted acid digestion with 3 mL H_2O_2 (30% *v/v*), 8 mL HNO_3 (65% *v/v*), and 2 mL HF (40% *v/v*), followed by a neutralization step with H_3BO_3 (4% *w/v*) (EN 15290:2011). The quantification of several metals and metalloids in the acidic eluates was performed by inductively coupled plasma atomic emission spectroscopy (ICP-AES).

The mobility of chemical species from the carbons was determined by a leaching test (EN 12457-2:2002): the adsorbents were mixed for 24 h with deionized water at 10 rpm, under a liquid/solid ratio of 10 L kg^{-1}, using a top-to-top shaker. At the end of the

stirring time, the mixtures were filtrated through cellulose nitrate membranes of 0.45 µm porosity. The resulting aqueous eluates were characterized for pH and several metals and metalloids using ICP-AES. The relative mobility of chemical elements was determined by Equation (1) [38]:

$$RM = \frac{C_{aqueous\ eluate}}{C_{acidic\ eluate}} \times 100 \quad (1)$$

where RM is the relative mobility of the chemical element (%), $C_{aqueous\ eluate}$ is the concentration of the chemical element in the aqueous eluate obtained in the leaching test (mg L^{-1}), and $C_{acidic\ eluate}$ is the concentration of the chemical element quantified in the bulk mineral content (mg L^{-1}).

The carbons were also analyzed by Fourier-transform infrared (FTIR) (Perkin-Elmer-Spectrum 1000 Spectrometer instrument), using the KBr disk method, to identify the functional groups on their surfaces. The textural properties were also characterized by using nitrogen (N_2) adsorption-desorption isotherms, at 77 K (Micromeritics ASAP2010). The samples were previously outgassed overnight at 150 °C under vacuum pressure. The surface area was determined through the Brunauer–Emmett–Teller (BET) equation by using a range of relative pressures (p/p_0) determined by the Rouquerol method [39]. The micropore volume was determined by the t-plot method. The total pore volume was determined from the amount of N_2 adsorbed at $p/p_0 = 0.95$. The mesopore volume was calculated by subtracting the micropore volume from the total pore volume.

2.3. Batch Adsorption Assays

The Cu^{2+} aqueous solutions were prepared by the dissolution of a 1000 mg Cu^{2+} L^{-1} stock solution, which was obtained from $CuSO_4.5H_2O$ salt (VETEC, p.a.) dissolved in ultrapure water (Milli-Q Academic, Millipore). The paracetamol aqueous solutions were prepared by dilution of a 1000 mg L^{-1} paracetamol standard solution. This standard solution was obtained by dissolution of the paracetamol pure compound (Sigma-Aldrich, Burlington, MA, USA, purity > 98%) in ultrapure water.

The adsorption experiments were carried out by mixing 10 mg of carbon with 20 mL of the adsorbate solution. Each batch adsorption assay was performed in duplicate. The kinetic and equilibrium studies were undertaken at the pH 3.00 adjusted by adding HNO_3 0.1–1.0 mol L^{-1}. The solid/liquid ratio as well as the solution pH used in the adsorption experiments were previously optimized in laboratory essays [37]. Doses of carbon below 10 mg provided very low removals of Cu ions. To avoid copper precipitation, pH conditions below 5 were used and a pH of 3 provided the highest copper removal with minimal precipitation.

The solutions containing the carbons were stirred at 150 rpm. At the end of the mixing period, the suspension was filtrated and the concentrations of paracetamol and Cu^{2+} in the filtrates were determined by UV-VIS spectrophotometry, at λ = 245 nm (HACH DR 5000), and ICP-AES, respectively.

The uptake capacity of paracetamol and Cu^{2+} was calculated from Equation (2):

$$q_t = \frac{C_0 - C_e}{M} \times V \quad (2)$$

where q_t is the uptake capacity (mg g^{-1}), C_0 and C_e are the initial and equilibrium concentrations, respectively, of paracetamol and Cu^{2+} (mg L^{-1}), M is the mass of adsorbent (g), and V is the solution volume (L).

2.4. Adsorption Experiments on the Single Component System—Kinetics

The kinetic runs on single-component systems were carried out with 50 mg L^{-1} of each adsorbate. Samples were taken between 5 to 1440 min at room temperature. The pH value was determined after each adsorption assay. Several models have been proposed to express the mechanism of kinetic removal. The most used ones are the pseudo-first-

order (PFO) kinetic model [40] (Equation (3)) and the pseudo-second-order (PSO) kinetic model [41] (Equation (4)):

$$q_t = q_e \left(1 - e^{-k_1 t}\right) \quad (3)$$

$$q_t = \frac{{q_e}^2 k_2 t}{1 + k_2 q_e t} \quad (4)$$

where q_t and q_e are the uptake capacities of paracetamol and Cu^{2+} (mg g^{-1}) at time t and equilibrium (min), respectively, k_1 is the rate constant of the PFO kinetic model (min^{-1}), and k_2 is the rate constant of the PSO kinetic model (g mg^{-1} h^{-1}).

The modeling of experimental data was performed using the OriginLab software. The experimental uptake capacities were compared to those calculated from the models by using the chi-square, χ^2, test according to Equation (5) [42]:

$$\chi^2 = \sum \frac{(q_e - q_{e,m})^2}{q_{e,m}} \quad (5)$$

where q_e is the experimental uptake capacity at equilibrium (mg g^{-1}) and $q_{e,m}$ is the modeled uptake capacity at equilibrium (mg g^{-1}).

The model for which Akaike Information Criterion (AIC) is a minimal value was selected as the ideal model that better describes the experimental data. AIC can be calculated by Equation (6) [43]:

$$AIC = 2k - 2\ln(L) \quad (6)$$

where L is the likelihood function and k is the number of estimated parameters.

2.5. Adsorption Experiments on the Binary Component System

The kinetic runs on the binary component system were conducted with mixed solutions of 50 mg L^{-1} Cu^{2+} + 50 mg L^{-1} paracetamol. The experimental conditions were the same used for the single system (time range of 5 min to 1440 min, 10 mg of carbon, 20 mL of solution, initial pH of 3 and room temperature). The kinetic data for binary adsorption were also modeled according to the kinetic models proposed for the single system.

For batch equilibrium experiments, the initial concentration of the two adsorbates was kept in the range of 5 mg L^{-1} to 250 mg L^{-1}.

The mechanism of binary adsorption may be quantitatively discussed through the effect of interaction (Equation (7)):

$$EI = \frac{q_{e,mix}}{q_e} \quad (7)$$

where EI is the effect of interaction (dimensionless), $q_{e,mix}$ is the uptake capacity of each adsorbate in equilibrium in the binary system (mg g^{-1}), and q_e is the uptake capacity of each adsorbate in equilibrium in the single system (mg g^{-1}).

Three types of effects may be observed: positive synergism ($EI > 1$), antagonism ($EI < 1$), and no interaction ($EI = 1$) [44,45].

2.6. Ecotoxicity Assessment

The ecotoxicity level of the aqueous eluates obtained in the leaching test of carbons and the aqueous solutions before and after binary adsorption assays was assessed by using the Microtox® assay (ISO 11348-3:2007). In this ecotoxicity assay, the bioluminescence inhibition of the *Vibrio fischeri* bacterium is evaluated after 30 min of exposure to the aqueous samples. The result is expressed as the effective concentration (% *v/v*) of the aqueous solution that induces a 50% decrease in the *V. fischeri* bioluminescence (EC_{50}-30 min) (% *v/v*). The lower the EC_{50} value, the higher the ecotoxicity level of the eluate for the bacterium. Control tests corresponding to paracetamol and Cu^{2+} in single and binary solutions with a concentration of 50 mg L^{-1} were also performed.

3. Results and Discussion

3.1. Characterization of the Carbons and Their Eluates

3.1.1. Proximate and Elemental Analyses and pHpzc

Table 1 presents the results of the proximate and elemental analyses as well as the pHpzc for all the carbons. The biomass-derived carbons showed very similar characteristics between them. The NOR carbon presented around twice the ash content and approximately half of the oxygen content of the biomass-derived carbons. These differences should be related to the precursors used in the production of the carbons: biomass for BBS and DND versus mineral coal for NOR. The values of pHpzc are neutral to slightly alkaline, which agrees with already reported results in the literature [7,9,46].

Table 1. Proximate and elemental analyses, and pHpzc of the three carbons.

Parameters	Carbons		
	BBS	DND	NOR
Proximate analysis [a] (% *w/w*)			
Moisture (%)	10.2	8.9	11.7
Volatile matter	8.6	11.7	7.0
Ashes	7.4	6.6	11.6
Fixed carbon	73.8	72.7	69.7
Elemental analysis [a] (% *w/w*)			
C	79.6	78.9	80.2
H	0.7	1.0	0.3
N	0.4	0.5	0.4
S	<0.03	<0.03	<0.03
O [b]	11.9	13.0	7.5
pHpzc	7.5	7.8	8.0

BBS: Babassu-derived carbon; DND: Dende-derived carbon; NOR: Commercial activated carbon; [a] as-received basis; [b] O = 100 − (C + H + N + S + Ashes).

3.1.2. Thermogravimetric Analysis

TGA curves of the carbons are shown in Figure S1 (Supplementary Material). All the samples presented high thermal stability with mass losses below 10% up to 850 °C. The mass loss at around 110 °C is due to the evaporation of water contained in the samples. The high thermal stability indicates that the biomass-derived carbons can be submitted to thermal regeneration.

3.1.3. Bulk Mineral Content

Table 2 shows the bulk mineral content of all activated carbons.

Table 2. Bulk mineral content (mg kg^{-1} db; $\overline{X} \pm \sigma$, $n = 3$ replicates) of the three carbons.

Chemical Element	Carbons		
	BBS	DND	NOR
Si	25,907 ± 554	17,521 ± 234	32,016 ± 120
K	6043 ± 467	5189 ± 113	623 ± 3.1
Fe	1323 ± 205	1692 ± 97	7255 ± 551
Ca	786 ± 3.4	1165 ± 61	1524 ± 35
Mg	749 ± 68	4525 ± 508	170 ± 29
Al	452 ± 63	1148 ± 32	13,473 ± 2006
Mn	49 ± 0.1	53 ± 0.2	30 ± 3.9

Table 2. *Cont.*

Chemical Element	Carbons		
	BBS	**DND**	**NOR**
Zn	35 ± 13	30 ± 3.5	20 ± 3.7
Na	23 ± 19	276 ± 13	257 ± 42
Cu	22 ± 0.3	45 ± 0.4	9.0 ± 0.1
Se	22 ± 0.1	<1.8	30 ± 0.2
Ba	13 ± 1.1	14 ± 0.3	70 ± 0.9
Pb	13 ± 0.3	<0.2	19 ± 1.9
As	<0.2	<0.2	31 ± 0.3
Ni	<1.5	<1.5	38 ± 0.3
Cr	<0.6	<0.6	11 ± 0.1
Mo	<0.2	<0.2	<0.2

The biomass-derived carbons presented high content of Si, K, Fe, Ca, and Mg, which was expected given their lignocellulosic origin. On the other hand, besides Si, Fe, and Ca, the NOR sample also presented high content of Al, which is related to its mineral origin. These results are in agreement with previous studies [37,38].

3.1.4. Mobility of Chemical Elements

Table 3 shows the chemical characterization of the eluates of the carbons obtained in the leaching test.

Table 3. Chemical characterization of the eluates (mg kg^{-1} db; $\overline{X} \pm \sigma$, n = 3 replicates) and relative mobility of chemical elements (%) of the three carbons.

Chemical Element	BBS		DND		NOR	
	Eluate Concentration	**Relative Mobility**	**Eluate Concentration**	**Relative Mobility**	**Eluate Concentration**	**Relative Mobility**
K	3221 ± 237	53.3	1262 ± 50	24.3	8.20 ± 0.30	1.31
Mg	69.0 ± 2.9	15.3	36.0 ± 3.4	0.800	5.30 ± 0.60	3.12
Ca	22.0 ± 1.9	2.80	0.700 ± 0.100	0.060	36.0 ± 1.0	2.36
Na	3.30 ± 0.40	14.4	30.0 ± 0.1	10.9	2.80 ± 0.10	1.09
Si	80.0 ± 0.3	0.310	123 ± 1	0.700	26.0 ± 1.1	0.008
Fe	0.060 ± 0.120	0.004	0.110 ± 0.080	0.006	0.090 ± 0.050	0.001
Al	<0.050	<0.010	<0.050	<0.004	0.550	0.004
Ba	<0.001	<0.007	<0.001	<0.007	<0.001	<0.001
Zn	<0.004	<0.010	<0.004	<0.010	<0.004	<0.02
Cu	<0.041	<0.180	<0.041	<0.090	<0.041	<0.45
Se	<0.053	<0.240	<0.053	n.a.	<0.053	<0.17
As	<0.005	n.a.	<0.005	n.a.	<0.005	<0.01
Ni	<0.043	n.a.	<0.043	n.a.	<0.043	<0.11
Pb	<0.005	<0.030	<0.005	n.a.	<0.005	<0.02
Cr	<0.018	n.a.	<0.018	n.a.	<0.018	<0.16
Mo	<0.006	n.a.	<0.006	n.a.	<0.006	n.a.
pH	7.8	n.a.	9.5	n.a.	7.9	n.a.

db: dry basis; n.a.: not applicable.

The BBS and DND had the highest mobility rates, indicating that a significant fraction of the metallic elements was present in the carbons as water-soluble salts [38,47,48]. Particularly, K was the ash-forming element that showed greater mobility during the leaching test for both BBS (53.3%) and DND (24.3%). Na element also presented significant mobility with mobility rates of 14.4% for BBS and 10.9% for DND. The BBS carbon also showed high mobility of Mg (15.3%). The higher mobility of these alkaline and alkaline-earth elements of the biomass-derived carbons might induce a cation-exchange mechanism in the adsorption

process. Other elements that were quantified in the carbons with high concentrations, such as Si, Fe, and Al, presented a low release or were not leached, suggesting that they are well immobilized in the carbon matrix. Overall, the NOR sample provided low mineral mobility suggesting that its minerals are well retained. All the eluates presented basic character, particularly the aqueous eluate from DND carbon.

3.1.5. Ecotoxicity Assessment of the Carbons

The EC_{50}–30 min of all carbon samples was >99.0% *v/v*, indicating a non-ecotoxic behavior. This result indicates that all the adsorbents did not mobilize chemical elements in acute toxic concentrations for the bacterium in the leaching test.

3.1.6. FTIR Spectra

Figure 1 displays the FTIR spectra of the three carbons BBS, DND, and NOR.

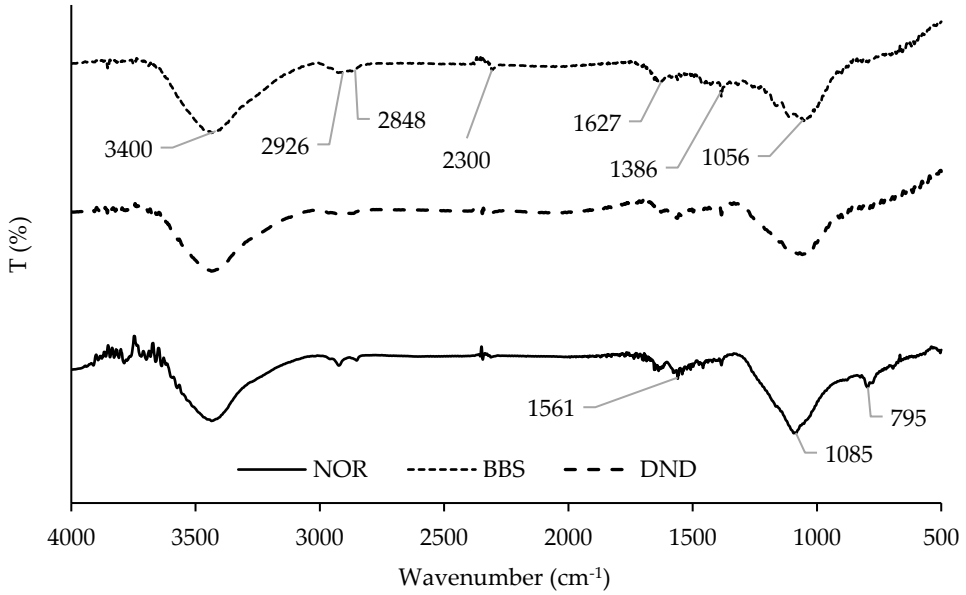

Figure 1. FTIR spectra of the three carbon samples (BBS: Babassu—derived carbon; DND: Dende—derived carbon; NOR: Commercial activated carbon).

The BBS and DND samples have similar bands because both are derived from lignocellulosic biowastes of the coconut fruits. A common band in the region of 3650–3200 cm^{-1} can be observed for all the spectra attributed to the stretching vibration of hydroxyl groups (O–H) of water, phenols, and alcohols [49,50]. The bands located between 2930–2800 cm^{-1} correspond to C–H stretching vibrations of methyl and/or methylene groups. Very small peaks at around 2307 cm^{-1} indicate stretching vibrations of the acetylenic group, C≡C [50,51].

The small peaks between 1626–1654 cm^{-1} for all spectra can be attributed to the C=O stretching vibrations of ketones, aldehydes, lactones, or carboxyl groups [51,52]. The band at 1560 cm^{-1} can be assigned to the C=C aromatic ring stretching vibrations [50]. The peaks around 1386 cm^{-1} can be attributed to the C–H stretching vibrations of aliphatic groups [49]. The peaks between 1030 cm^{-1} and 1170 cm^{-1} can be associated with the C-O stretching of alcohols and/or phenols and/or the stretching vibration of C–O–C from ethers [49].

3.1.7. Textural Properties of the Carbon Samples

The N_2 adsorption-desorption isotherms (Figure S2, Supplementary Material) of BBS and DND samples are of type I (a) according to IUPAC classification [53]. These isotherms are typical of microporous materials having mainly narrow micropores (width < ≈ 1 nm).

NOR sample shows an isotherm of type I(b), which is typical of microporous materials with an enlarged distribution of pore sizes including micropores and narrow mesopores (< ≈2.5 nm).

The textural data obtained from the N_2 physisorption analysis are shown in Table 4.

Table 4. Textural properties of the three activated carbons.

Carbon	S_{BET} (m^2 g^{-1})	V_{total} (cm^3 g^{-1})	V_{mes} (cm^3 g^{-1})	V_{micro} (cm^3 g^{-1})
BBS	784	0.34	0.08	0.26
DND	767	0.34	0.09	0.25
NOR	1083	0.57	0.41	0.16

S_{BET}: surface area; V_{total}: total pore volume; V_{mes}: mesopore volume; V_{micro}: micropore volume.

BBS and DND carbons showed relatively high surface area (S_{BET}) associated with their high volume of micropores. The values are close to those found in the literature for babassu (S_{BET} of 624, 625, and 688 mg^2 g^{-1} according to [7,51,54]) and dende carbons (S_{BET} of 672 mg^2 g^{-1} according to [11]). The NOR carbon shows the highest S_{BET} with 1083 m^2 g^{-1}, although it presents a smaller micropore volume but a much higher mesopore volume.

3.2. Adsorption in Single and Binary Systems: Kinetics, Equilibrium Assays, and Ecotoxicity

3.2.1. Adsorption Kinetics

Results for single and binary adsorption experiments are shown in Figure S3. The experimental data were adjusted to PFO and PSO kinetic models, and the best model was selected according to the highest determination coefficient (R^2), lower χ^2 value, and lower AIC value.

For both the single and binary systems and all the adsorbents, the best fitting was obtained with the PSO model. The calculated parameters (experimental and modeled with the PSO kinetic model) are summarized in Table S1 (Supplementary Material).

The single paracetamol adsorption (Figure 2A,D,G) shows a kinetic equilibrium occurring at around 300 min, for BBS and DND carbons, and 60 min for the NOR carbon. The fastest adsorption associated with NOR carbon is related to the higher mesopore content of this sample (Table 4). The experimental maximum uptake capacities of paracetamol were 90.4 mg g^{-1} for BBS, 94.2 mg g^{-1} for DND, and 95.2 mg g^{-1} for the NOR sample. Despite the different surface areas of biowaste-derived carbons and commercial carbon, the paracetamol uptake capacity was quite similar for all samples indicating a strong influence of the pore size, particularly the micropore size as it was pointed out by Cabrita et al. (2010) [55].

The carbons' surfaces are positively charged since the pH_{PZC} values are quite above the solution pH of 3.0 (Table 1), and the paracetamol molecule is in its protonated form (pKa ≈ 9.0); therefore, electrostatic interactions between the molecule and the carbons' surface are not not expected. The π-π bonding between the aromatic rings of the carbons and the aromatic ring of the organic molecule, as well as hydrogen bonding, might have been responsible for the paracetamol removal from the single and binary solutions [56,57].

Figure 2B,E,H show that Cu^{2+} adsorption is very rapid within the first 30 min and then the equilibrium is reached. This behavior is due to the few sites available for Cu^{2+} adsorption. Although the biowaste carbons presented some K, Na, and Mg mobility (Table 3) that may have played a role in the cation exchange mechanism, the Cu^{2+} uptake was low. Complexation of Cu^{2+} by oxygenated functional groups at carbons' surface is another possibility since the importance of hydroxyl groups in Cu removal was previously demonstrated [58–60]. As shown in FTIR spectra (Figure 1), hydroxyl groups are effectively present at carbons' surface.

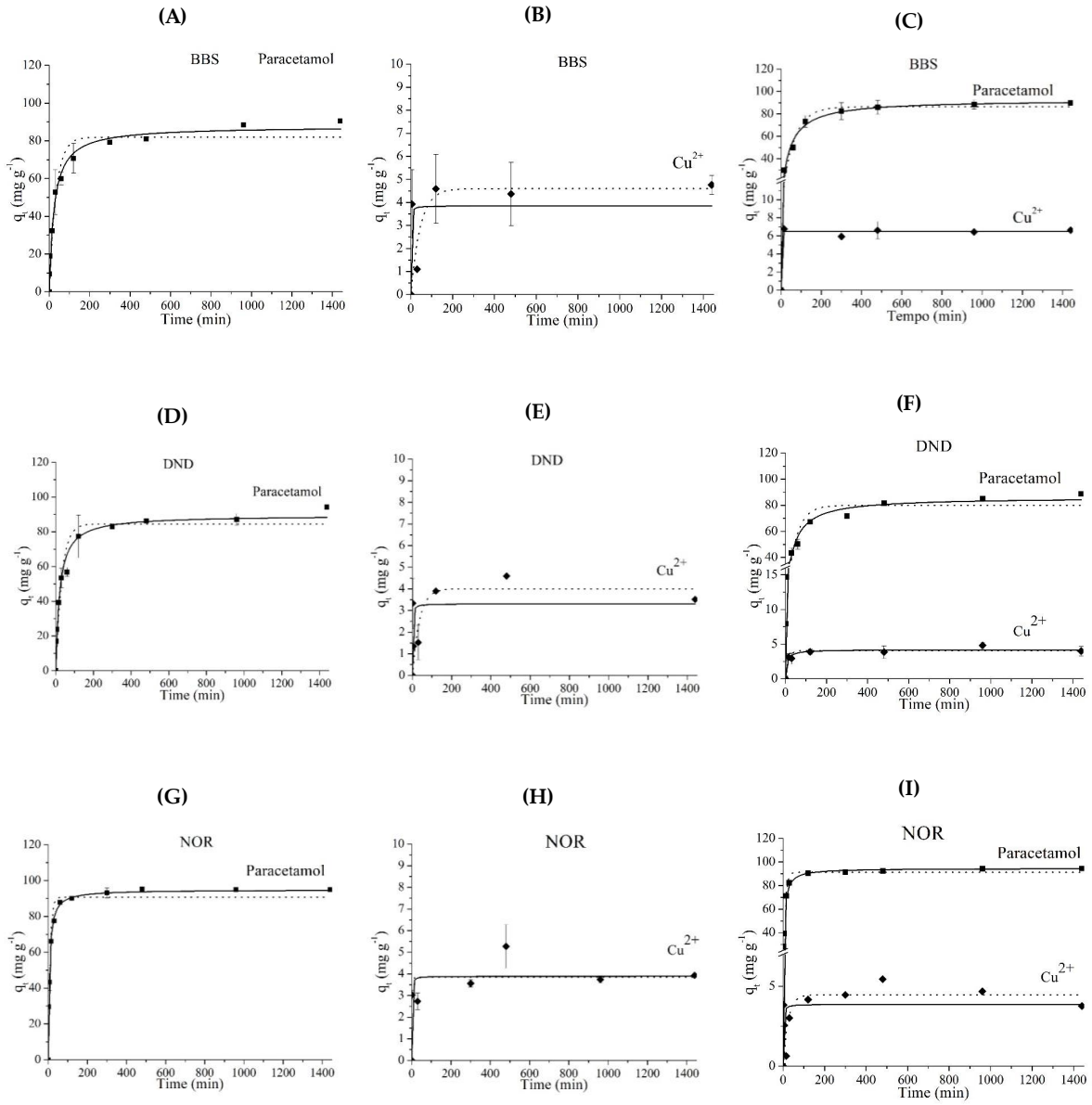

Figure 2. Kinetic data from single and binary adsorption systems with the carbons BBS ((**A**): single paracetamol, (**B**): single Cu^{2+}; (**C**): binary system with paracetamol and Cu^{2+}), DND ((**D**): single paracetamol, (**E**): single Cu^{2+}; (**F**): binary system with paracetamol and Cu^{2+}), and NOR ((**G**): single paracetamol, (**H**): single Cu^{2+}; (**I**): binary system with paracetamol and Cu^{2+}); (solid line) PFO and (dotted line) PSO non—linear fitting; dots—experimental points.

Figure 2C,F,I depict the adsorption in binary systems. Compared to the single systems, no relevant changes in the kinetic curves and equilibrium times have been registered. Thus, no collaborative or competitive adsorption was found for both the metal ion and pharmaceutical molecule, indicating that Cu^{2+} and paracetamol adsorption was site-specific.

The lack of competition between paracetamol and Cu^{2+} was also confirmed for single and binary systems with a higher concentration of paracetamol and Cu^{2+} (100 mg L^{-1} Cu^{2+} + 100 mg L^{-1} paracetamol.) Table 5 shows the uptake capacities for paracetamol and Cu^{2+} in single and binary systems for each carbon, as well as the Effect of Interaction (EI).

Table 5. Uptake capacities and EI on the adsorption process of paracetamol and Cu^{2+} in single and binary systems under an initial concentration of 100 mg L^{-1} for each adsorbate.

Carbon	Paracetamol			Cu^{2+}		
	q_e Single (mg g^{-1})	q_e Binary (mg g^{-1})	EI	q_e Single (mg g^{-1})	q_e Binary (mg g^{-1})	EI
BBS	98.4	97.8	0.99	15.0	12.2	0.81
DND	109	104	0.95	16.6	15.7	0.94
NOR	123	115	0.93	18.1	16.2	0.89

The EI values are quite close to 1.0, meaning that no significant interaction exists between paracetamol and Cu^{2+} even for the double of the concentration tested in the kinetic study.

3.2.2. Equilibrium Studies—Adsorption Isotherms

Since there was no interaction between paracetamol and Cu^{2+}, the adsorption isotherms were only determined for the binary systems. The obtained results were fitted to the widely used Langmuir and Freundlich models [61,62] (Figure S3, Supplementary Material). The isotherms are convex, revealing a favorable adsorption process. In addition, the isotherms can be classified as type L [63], where adsorption increases markedly under low equilibrium concentrations and reaches a plateau after continuously increasing equilibrium concentration.

Table 6 shows that the Langmuir model obtained the best fit for paracetamol in the binary system for all adsorbents, while for Cu^{2+}, the Freundlich model showed the best fit. The Langmuir model is associated with the monolayer adsorption concept assuming that once an adsorbate molecule occupies a site, no further adsorption can take place at that site and no interaction occurs between the molecules adsorbed on and the adjacent or nearby sites. On the other hand, the Freundlich model conceives an energetic heterogeneity of the active sites, considering multilayer formation.

Table 6. Langmuir and Freundlich parameters for paracetamol and Cu^{2+} adsorption in binary systems.

Adsorbent	Isotherm Model	Parameters	Paracetamol Binary	Cu^{2+} Binary
BBS	Langmuir	q_e exp	115	10.7
		q_{max}	128	12.2
		K_L	0.090	0.090
		R^2	0.880	0.846
		AIC	61.4	16.8
	Freundlich	K_F	26.4	3.65
		1/n	0.343	0.248
		R^2	0.816	0.850
		AIC	57.5	17.1
DND	Langmuir	q_e exp	104	15.7
		q_{max}	149	16.6
		K_L	0.070	0.160
		R^2	0.921	0.971
		AIC	48.8	10.5
	Freundlich	K_F	16.4	5.18
		1/n	0.523	0.263
		R^2	0.837	0.973
		AIC	54.6	10.7

Table 6. *Cont.*

Adsorbent	Isotherm Model	Parameters	Paracetamol Binary	Cu^{2+} Binary
NOR	Langmuir	q_e exp	132	17.8
		q_{max}	148	20.2
		K_L	0.115	0.058
		R^2	0.952	0.949
		AIC	51.4	14.7
	Freundlich	K_F	30.3	3.19
		1/n	0.362	0.389
		R^2	0.881	0.962
		AIC	59.9	12.3

q_e exp: experimental uptake capacity in mg g^{-1}; q_{max}: maximum uptake capacity in mg g^{-1}; K_L: Langmuir constant in L mg^{-1}; K_F: Freundlich constant in (mg g^{-1})(mg L^{-1})^n; 1/n: dimensionless adsorption intensity.

Considering the obtained results, the DND carbon presented the highest affinity for Cu^{2+} (highest K_F), while the BBS showed the second highest affinity for paracetamol quite close to the NOR activated carbon.

3.2.3. Ecotoxicity

Ecotoxicity tests were also performed in the adsorbates' solutions at a pH of 3.0 (natural solutions' pH) and the optimum pH for *V. fischeri* bacterium (pH = 8.0). These results were previously reported [37]. The single paracetamol solution (50 mg L^{-1}), at pH 3.0, presented an EC_{50}-30 min of 14.8% *v/v* showing a high ecotoxic level. When the pH was adjusted for 8.0, the EC_{50}-30 min increased to 21.7% indicating a small decrease in the toxicity, but it is still a relevant effect on *V. fischeri*. The literature is quite variable presenting very different EC_{50} values for paracetamol [64–66].

The single Cu^{2+} solution (50 mg L^{-1}), at pH 3.0, showed an EC_{50}-30 min < 2.5% *v/v*, indicating a very high toxicity level. In fact, the high toxicity of Cu ions for *V. fischeri* at low concentrations was reported in the literature [67]. After the pH correction to 8.0, the toxicity for the bacterium was not detectable (EC_{50}-30 min > 99% *v/v*). The toxicity was probably due not only to the Cu^{2+} but also to the natural pH of the solution. Considering that Cu^{2+} ions form insoluble hydroxides when pH > 5, the pH correction to a value of 8.0 precipitated the Cu present in the solution, decreasing its toxicity level to the bacterium [68].

For the paracetamol and Cu^{2+} binary solution (50 mg L^{-1} + 50 mg L^{-1}), at both pH 3.0 and pH = 8.0, the ecotoxic level was quite high (EC_{50}-30 min < 2.5% *v/v*), indicating that the simultaneous presence of these substances may have a synergistic toxic effect to *V. fischeri.*

The ecotoxicity evaluation after adsorption on the binary systems before pH correction (final pH = 3.0) provided an EC_{50}-30 min of <2.5% *v/v* for the aqueous solutions, indicating a high acute toxicity level for *Vibrio fischeri*. After the pH correction (final pH = 8.0), the EC_{50}-30 min increased dramatically to a non-toxic level (>99% *v/v*), resulting from the large removal of paracetamol, since the pharmaceutical molecule presented an EC_{50}-30 min of 21.7% *v/v* by itself. This result differs from the ones obtained by Ferreira et al. (2022) [37], where the binary mixture of paracetamol + Cu^{2+} still presented high toxicity after adsorption due to a low removal of paracetamol. This result demonstrates the importance of the high-efficiency removal of paracetamol from the aqueous solutions to decrease their acute toxicity levels.

4. Conclusions

The characterizations performed on the carbons allowed concluding that although the CC sample presented a higher surface area (S_{BET} = 1083 m^2/g), the porous carbons derived from the biowastes were richer in micropores (V_{micro} = 0.25—0.26 cm^3/g), while the CC carbon presented wider pore size distribution with a higher mesopore volume (V_{meso} = 0.41 cm^3/g). Regarding the surface chemistry, all the carbons presented a slightly

alkaline behavior with pHpzc values between 7.0 and 8.0. The biowaste-derived carbons presented high concentrations of metallic elements such as Si, K, Ca, and Mg, while the commercial carbon presented high content of Si, Al, and Fe. The mobility of the K element was significant in the biowaste-derived carbons while the commercial sample showed that its metallic elements are well immobilized in the carbonaceous matrix. The ecotoxicity assessment indicated a non-ecotoxic behavior for all the carbons (EC_{50}-30 min > 99% *v/v*). While the bicomponent solution presented a high ecotoxicity (EC_{50}-30 min < 2.5% *v/v*) before adsorption, the EC_{50}-30 min increased dramatically to a non-toxic level (>99% *v/v*) after adsorption, resulting from the large removal of paracetamol.

No significant competition between the adsorbates was observed in the bicomponent solutions adsorption experiments since the uptake capacities obtained were similar to the ones obtained in the monocomponent solutions, indicating that paracetamol and Cu^{2+} adsorption was site-specific.

Paracetamol adsorption was related to the micropore filling, π-π interactions, and H-bonding, whereas Cu^{2+} removal was attributed to the cation exchange mechanism and complexation with the hydroxyl groups at the carbons' surface.

This work demonstrates that it is possible to valorize babassu and dende byproducts produced at oil plants as carbons with high efficiency in the removal of paracetamol and Cu^{2+} from aqueous solutions. Further studies on the application of these biowaste-derived carbons in real wastewater matrices are required.

Supplementary Materials: The following supporting information can be downloaded at: https://www.mdpi.com/article/10.3390/pr11072146/s1, Figure S1: TGA curves of the carbons (BBS: babassu−derived carbon; DND: Dende−derived carbon; NOR: Commercial activated carbon).; Figure S2: N_2 adsorption−desorption isotherms at 77 K of the carbons (BBS: babassu−derived carbon; DND: Dende−derived carbon; NOR: Commercial activated carbon); Figure S3: Experimental data and fitting to the Langmuir and Freundlich isotherm models for paracetamol and Cu^{2+} adsorption in binary systems (A, C, and E: paracetamol adsorption in a binary system with BBS, DND, and NOR, respectively; B, D, and F: Cu^{2+} adsorption in a binary system with BBS, DND, and NOR, respectively; BBS: babassu; DND: Dende; NOR: Norit); Table S1: Kinetic parameters from PSO kinetic model for single and binary adsorption experiments.

Author Contributions: Conceptualization, N.L., M.B. and M.A.S.D.d.B.; methodology, R.C.F. and D.D., N.L., M.B. and M.A.S.D.d.B.; validation, N.L., M.B., T.P.d.A. and M.A.S.D.d.B.; formal analysis, N.L., M.B., T.P.d.A. and M.A.S.D.d.B.; investigation, R.C.F., D.D., N.L., M.B., T.P.d.A. and M.A.S.D.d.B.; resources, N.L., M.A.S.D.d.B. and I.M.F.; writing—original draft preparation, R.C.F.; writing—review and editing, N.L., M.B., T.P.d.A., M.A.S.D.d.B. and I.M.F.; visualization, R.C.F. and M.B.; supervision, N.L., M.A.S.D.d.B. and I.M.F.; project administration, N.L. and M.A.S.D.d.B.; funding acquisition, N.L., M.A.S.D.d.B. and I.M.F. All authors have read and agreed to the published version of the manuscript.

Funding: This study was financially supported by the National Council for Scientific and Technological Development (CNPq) and the Coordination for the Improvement of Higher Level (CAPES) by the CAPES/Chemical Engineering Department/process 88881.135075/2016-01. The authors also acknowledge the LGCPA/UEM. This work was also supported by the Associate Laboratory for Green Chemistry—LAQV, which is financed by national funds from FCT/MCTES (UIDB/50006/2020 and UIDP/50006/2020). Maria Bernardo thanks FCT (Fundação para a Ciência e Tecnologia) for funding through program DL 57/2016—Norma transitória.

Data Availability Statement: Not applicable.

Conflicts of Interest: The authors declare no conflict of interest.

References

1. Companhia Nacional de Abastecimento (CONAB). *Boletim da Sociobiodiversidade*; CONAB: Brasilia, Brazil, 2022.
2. Carrazza, L.R.; Ávila, J.C.C.; da Silva, M.L. *Manual Tecnológico de Aproveitamento Integral do Fruto do Babaçu*; ISPN: Brasilia, Brazil, 2012.

3. USDA Palm Oil Explorer. Available online: https://ipad.fas.usda.gov/cropexplorer/cropview/commodityView.aspx?cropid=4243000 (accessed on 18 May 2023).
4. Cardoso Vieira, M.; Pischke Garske, R.; de Souza Rocha, P.; da Fontoura Xavier Costa, L.; Nunes Paiva, A.R.; Thys, R.C.S. Babassu Mesocarp Flour: A Nutritive Brazilian By-product for Gluten-free Muffins. *J. Culin. Sci. Technol.* **2021**, *21*, 517–532. [CrossRef]
5. Kaniapan, S.; Hassan, S.; Ya, H.; Patma Nesan, K.; Azeem, M. The Utilisation of Palm Oil and Oil Palm Residues and the Related Challenges as a Sustainable Alternative in Biofuel, Bioenergy, and Transportation Sector: A Review. *Sustainability* **2021**, *13*, 3110. [CrossRef]
6. Ferreira, R.C.; Couto, O.M.; Carvalho, K.Q.; Arroyo, P.A.; Barros, M.A.S.D. Effect of solution pH on the removal of paracetamol by activated carbon of dende coconut mesocarp. *Chem. Biochem. Eng. Q.* **2015**, *29*, 47–53. [CrossRef]
7. Hoppen, M.I.; Carvalho, K.Q.; Ferreira, R.C.; Passig, F.H.; Pereira, I.C.; Rizzo-Domingues, R.C.P.; Lenzi, M.K.; Bottini, R.C.R. Adsorption and desorption of acetylsalicylic acid onto activated carbon of babassu coconut mesocarp. *J. Environ. Chem. Eng.* **2019**, *7*, 102862. [CrossRef]
8. Vilella, P.C.; Lira, J.A.; Azevedo, D.C.S.; Bastos-Neto, M.; Stefanutti, R. Preparation of biomass-based activated carbons and their evaluation for biogas upgrading purposes. *Ind. Crops Prod.* **2017**, *109*, 134–140. [CrossRef]
9. Melo, L.L.A.; Ide, A.H.; Duarte, J.L.S.; Zanta, C.L.P.S.; Oliveira, L.M.T.M.; Pimentel, W.R.O.; Meili, L. Caffeine removal using Elaeis guineensis activated carbon: Adsorption and RSM studies. *Environ. Sci. Pollut. Res.* **2020**, *27*, 27048–27060. [CrossRef]
10. Lai, J.Y.; Ngu, L.H.; Hashim, S.S.; Chew, J.J.; Sunarso, J. Review of oil palm-derived activated carbon for CO_2 capture. *Carbon Lett.* **2021**, *31*, 201–252. [CrossRef]
11. Ferreira, R.C.; de Lima, H.H.C.; Cândido, A.A.; Junior, O.M.C.; Arroyo, P.A.; Gauze, G.F.; Carvalho, K.Q.; Barros, M.A.S.D. Adsorption of Paracetamol Using Activated Carbon of Dende and Babassu Coconut Mesocarp. *Int. J. Biol. Biomol. Agric. Food Biotechnol. Eng.* **2015**, *9*, 575–580.
12. Zbair, M.; Ait Ahsaine, H.; Anfar, Z. Porous carbon by microwave assisted pyrolysis: An effective and low-cost adsorbent for sulfamethoxazole adsorption and optimization using response surface methodology. *J. Clean. Prod.* **2018**, *202*, 571–581. [CrossRef]
13. Jaria, G.; Silva, C.P.; Oliveira, J.A.B.P.; Santos, S.M.; Gil, M.V.; Otero, M.; Calisto, V.; Esteves, V.I. Production of highly efficient activated carbons from industrial wastes for the removal of pharmaceuticals from water—A full factorial design. *J. Hazard. Mater.* **2019**, *370*, 212–218. [CrossRef]
14. To, M.-H.; Hadi, P.; Hui, C.-W.; Lin, C.S.K.; McKay, G. Mechanistic study of atenolol, acebutolol and carbamazepine adsorption on waste biomass derived activated carbon. *J. Mol. Liq.* **2017**, *241*, 386–398. [CrossRef]
15. Ahmed, M.J. Adsorption of non-steroidal anti-inflammatory drugs from aqueous solution using activated carbons: Review. *J. Environ. Manag.* **2017**, *190*, 274–282. [CrossRef]
16. Michelon, A.; Bortoluz, J.; Raota, C.S.; Giovanela, M. Agro-industrial residues as biosorbents for the removal of anti-inflammatories from aqueous matrices: An overview. *Environ. Adv.* **2022**, *9*, 100261. [CrossRef]
17. Mansour, F.; Al-Hindi, M.; Yahfoufi, R.; Ayoub, G.M.; Ahmad, M.N. The use of activated carbon for the removal of pharmaceuticals from aqueous solutions: A review. *Rev. Environ. Sci. Bio/Technol.* **2018**, *17*, 109–145. [CrossRef]
18. Kumar, M.; Ngasepam, J.; Dhangar, K.; Mahlknecht, J.; Manna, S. Critical review on negative emerging contaminant removal efficiency of wastewater treatment systems: Concept, consistency and consequences. *Bioresour. Technol.* **2022**, *352*, 127054. [CrossRef] [PubMed]
19. Patel, M.; Kumar, R.; Kishor, K.; Mlsna, T.; Pittman, C.U.; Mohan, D. Pharmaceuticals of Emerging Concern in Aquatic Systems: Chemistry, Occurrence, Effects, and Removal Methods. *Chem. Rev.* **2019**, *119*, 3510–3673. [CrossRef] [PubMed]
20. Ziylan-Yavas, A.; Santos, D.; Flores, E.M.M.; Ince, N.H. Pharmaceuticals and personal care products (PPCPs): Environmental and public health risks. *Environ. Prog. Sustain. Energy* **2022**, *41*, e13821. [CrossRef]
21. Madikizela, L.M.; Ncube, S. Health effects and risks associated with the occurrence of pharmaceuticals and their metabolites in marine organisms and seafood. *Sci. Total Environ.* **2022**, *837*, 155780. [CrossRef]
22. Tran, N.H.; Reinhard, M.; Gin, K.Y.-H. Occurrence and fate of emerging contaminants in municipal wastewater treatment plants from different geographical regions-a review. *Water Res.* **2018**, *133*, 182–207. [CrossRef]
23. Balakrishna, K.; Rath, A.; Praveenkumarreddy, Y.; Guruge, K.S.; Subedi, B. A review of the occurrence of pharmaceuticals and personal care products in Indian water bodies. *Ecotoxicol. Environ. Saf.* **2017**, *137*, 113–120. [CrossRef]
24. Carvalho, A.P.; Mestre, A.S.; Haro, M.; Ania, C.O. Advanced Methods for the Removal of Acetaminophen from Water. In *Acetaminophen: Properties, Clinical Uses, and Adverse Effects*; Javaherian, A., Latifpour, P., Eds.; Nova Publishers: New York, NY, USA, 2011; ISBN 9781619423749.
25. Żur, J.; Piński, A.; Marchlewicz, A.; Hupert-Kocurek, K.; Wojcieszyńska, D.; Guzik, U. Organic micropollutants paracetamol and ibuprofen—Toxicity, biodegradation, and genetic background of their utilization by bacteria. *Environ. Sci. Pollut. Res.* **2018**, *25*, 21498–21524. [CrossRef] [PubMed]
26. Parolini, M. Toxicity of the Non-Steroidal Anti-Inflammatory Drugs (NSAIDs) acetylsalicylic acid, paracetamol, diclofenac, ibuprofen and naproxen towards freshwater invertebrates: A review. *Sci. Total Environ.* **2020**, *740*, 140043. [CrossRef]
27. Rocha, C.H.B.; Costa, H.F.; Azevedo, L.P. Heavy metals in the São Mateus Stream Basin, Peixe River Basin, Paraiba do Sul River Basin, Brazil. *Ambient. Agua-Interdiscip. J. Appl. Sci.* **2019**, *14*, e2329. [CrossRef]
28. Saha, P.; Paul, B. Assessment of heavy metal toxicity related with human health risk in the surface water of an industrialized area by a novel technique. *Hum. Ecol. Risk Assess. Int. J.* **2019**, *25*, 966–987. [CrossRef]

29. Vareda, J.P.; Valente, A.J.M.; Durães, L. Assessment of heavy metal pollution from anthropogenic activities and remediation strategies: A review. *J. Environ. Manag.* **2019**, *246*, 101–118. [CrossRef]
30. Couto, C.M.C.M.; Ribeiro, C. Pollution status and risk assessment of trace elements in Portuguese water, soils, sediments, and associated biota: A trend analysis from the 80s to 2021. *Environ. Sci. Pollut. Res.* **2022**, *29*, 48057–48087. [CrossRef] [PubMed]
31. Rehman, M.; Liu, L.; Wang, Q.; Saleem, M.H.; Bashir, S.; Ullah, S.; Peng, D. Copper environmental toxicology, recent advances, and future outlook: A review. *Environ. Sci. Pollut. Res.* **2019**, *26*, 18003–18016. [CrossRef] [PubMed]
32. Thompson, L.J. Copper. In *Veterinary Toxicology*; Gupta, R.C., Ed.; Elsevier: Amsterdam, The Netherlands, 2018; pp. 425–427. ISBN 9780128114100.
33. Luo, C.-H.; Wang, R.; Zhao, Y.; Huang, J.; Evans, N.J. Mobilization of Cu in the continental lower crust: A perspective from Cu isotopes. *Geosci. Front.* **2023**, *14*, 101590. [CrossRef]
34. Zheng, J.; Li, Q.; Zheng, X. Ocean acidification increases copper accumulation and exacerbates copper toxicity in *Amphioctopus fangsiao* (Mollusca: Cephalopoda): A potential threat to seafood safety. *Sci. Total Environ.* **2023**, *891*, 164473. [CrossRef]
35. Quesada, H.B.; Baptista, A.T.A.; Cusioli, L.F.; Seibert, D.; de Oliveira Bezerra, C.; Bergamasco, R. Surface water pollution by pharmaceuticals and an alternative of removal by low-cost adsorbents: A review. *Chemosphere* **2019**, *222*, 766–780. [CrossRef]
36. Ahmed, M.J.; Hameed, B.H. Insights into the isotherm and kinetic models for the coadsorption of pharmaceuticals in the absence and presence of metal ions: A review. *J. Environ. Manag.* **2019**, *252*, 109617. [CrossRef] [PubMed]
37. Ferreira, R.C.; Dias, D.; Fonseca, I.; Bernardo, M.; Willimann Pimenta, J.L.C.; Lapa, N.; de Barros, M.A.S.D. Multi-component adsorption study by using bone char: Modelling and removal mechanisms. *Environ. Technol.* **2022**, *43*, 789–804. [CrossRef] [PubMed]
38. Dias, D.; Lapa, N.; Bernardo, M.; Godinho, D.; Fonseca, I.; Miranda, M.; Pinto, F.; Lemos, F. Properties of chars from the gasification and pyrolysis of rice waste streams towards their valorisation as adsorbent materials. *Waste Manag.* **2017**, *65*, 186–194. [CrossRef] [PubMed]
39. Rouquerol, J.; Llewellyn, P.; Rouquerol, F. Is the bet equation applicable to microporous adsorbents? In *Studies in Surface Science and Catalysis*; Llewellyn, P.L., Rodriquez-Reinoso, F., Rouqerol, J., Eds.; Elsevier: Amsterdam, The Netherlands, 2007; pp. 49–56. ISBN 9780444520227.
40. Lagergren, S. About the theory of so-called adsorption of soluble substances. *Sven. Vetensk. Handl.* **1898**, *24*, 1–39.
41. Ho, Y. Review of second-order models for adsorption systems. *J. Hazard. Mater.* **2006**, *136*, 681–689. [CrossRef] [PubMed]
42. Ho, Y.-S. Selection of optimum sorption isotherm. *Carbon N. Y.* **2004**, *42*, 2115–2116. [CrossRef]
43. Akaike, H. A new look at the statistical model identification. *IEEE Trans. Automat. Contr.* **1974**, *19*, 716–723. [CrossRef]
44. Agarwal, B.; Balomajumder, C.; Thakur, P.K. Simultaneous co-adsorptive removal of phenol and cyanide from binary solution using granular activated carbon. *Chem. Eng. J.* **2013**, *228*, 655–664. [CrossRef]
45. Mohan, D.; Singh, K.P. Single- and multi-component adsorption of cadmium and zinc using activated carbon derived from bagasse—An agricultural waste. *Water Res.* **2002**, *36*, 2304–2318. [CrossRef]
46. Couto, O.M.; Matos, I.; da Fonseca, I.M.; Arroyo, P.A.; da Silva, E.A.; de Barros, M.A.S.D. Effect of solution pH and influence of water hardness on caffeine adsorption onto activated carbons. *Can. J. Chem. Eng.* **2015**, *93*, 68–77. [CrossRef]
47. Dias, D.; Lapa, N.; Bernardo, M.; Ribeiro, W.; Matos, I.; Fonseca, I.; Pinto, F. Cr(III) removal from synthetic and industrial wastewaters by using co-gasification chars of rice waste streams. *Bioresour. Technol.* **2018**, *266*, 139–150. [CrossRef]
48. Dias, D.; Bernardo, M.; Matos, I.; Fonseca, I.; Pinto, F.; Lapa, N. Activation of co-pyrolysis chars from rice wastes to improve the removal of Cr3+ from simulated and real industrial wastewaters. *J. Clean. Prod.* **2020**, *267*, 121993. [CrossRef]
49. Coates, J. Interpretation of Infrared Spectra, A Practical Approach. In *Encyclopedia of Analytical Chemistry*; John Wiley & Sons, Ltd.: Chichester, UK, 2006.
50. Silverstein, R.M.; Webster, F.X.; Kiemle, D. *Spectrometric Identification of Organic Compounds*, 7th ed.; John Wiley & Sons: Hoboken, NJ, USA, 2005; ISBN 1118311655.
51. Ghosh, A.; da Silva Santos, A.M.; Cunha, J.R.; Dasgupta, A.; Fujisawa, K.; Ferreira, O.P.; Lobo, A.O.; Terrones, M.; Terrones, H.; Viana, B.C. CO_2 Sensing by in-situ Raman spectroscopy using activated carbon generated from mesocarp of babassu coconut. *Vib. Spectrosc.* **2018**, *98*, 111–118. [CrossRef]
52. Socrates, G. *Infrared and Raman Characteristic Group Frequencies: Tables and Charts*, 3rd ed.; John Wiley & Sons: Hoboken, NJ, USA, 2004; ISBN 0470093072.
53. Thommes, M.; Kaneko, K.; Neimark, A.V.; Olivier, J.P.; Rodriguez-Reinoso, F.; Rouquerol, J.; Sing, K.S.W. Physisorption of gases, with special reference to the evaluation of surface area and pore size distribution (IUPAC Technical Report). *Pure Appl. Chem.* **2015**, *87*, 1051–1069. [CrossRef]
54. Reck, I.M.; Paixão, R.M.; Bergamasco, R.; Vieira, M.F.; Vieira, A.M.S. Removal of tartrazine from aqueous solutions using adsorbents based on activated carbon and Moringa oleifera seeds. *J. Clean. Prod.* **2018**, *171*, 85–97. [CrossRef]
55. Cabrita, I.; Ruiz, B.; Mestre, A.S.; Fonseca, I.M.; Carvalho, A.P.; Ania, C.O. Removal of an analgesic using activated carbons prepared from urban and industrial residues. *Chem. Eng. J.* **2010**, *163*, 249–255. [CrossRef]
56. Bernal, V.; Erto, A.; Giraldo, L.; Moreno-Piraján, J. Effect of Solution pH on the Adsorption of Paracetamol on Chemically Modified Activated Carbons. *Molecules* **2017**, *22*, 1032. [CrossRef] [PubMed]

57. Nguyen, D.T.; Tran, H.N.; Juang, R.-S.; Dat, N.D.; Tomul, F.; Ivanets, A.; Woo, S.H.; Hosseini-Bandegharaei, A.; Nguyen, V.P.; Chao, H.-P. Adsorption process and mechanism of acetaminophen onto commercial activated carbon. *J. Environ. Chem. Eng.* **2020**, *8*, 104408. [CrossRef]
58. Chao, H.P.; Chang, C.C. Adsorption of copper(II), cadmium(II), nickel(II) and lead(II) from aqueous solution using biosorbents. *Adsorption* **2012**, *18*, 395–401. [CrossRef]
59. Kołodyńska, D.; Krukowska, J.; Thomas, P. Comparison of sorption and desorption studies of heavy metal ions from biochar and commercial active carbon. *Chem. Eng. J.* **2017**, *307*, 353–363. [CrossRef]
60. Li, A.Y.; Deng, H.; Jiang, Y.H.; Ye, C.H.; Yu, B.G.; Zhou, X.L.; Ma, A.Y. Superefficient Removal of Heavy Metals from Wastewater by Mg-Loaded Biochars: Adsorption Characteristics and Removal Mechanisms. *Langmuir* **2020**, *36*, 9160–9174. [CrossRef] [PubMed]
61. Wang, J.; Guo, X. Adsorption isotherm models: Classification, physical meaning, application and solving method. *Chemosphere* **2020**, *258*, 127279. [CrossRef] [PubMed]
62. Al-Ghouti, M.A.; Da'ana, D.A. Guidelines for the use and interpretation of adsorption isotherm models: A review. *J. Hazard. Mater.* **2020**, *393*, 122383. [CrossRef] [PubMed]
63. Giles, C.H.; MacEwan, T.H.; Nakhwa, S.N.; Smith, D. Studies in adsorption. Part XI. A system of classification of solution adsorption isotherms, and its use in diagnosis of adsorption mechanisms and in measurement of specific surface areas of solids. *J. Chem. Soc.* **1960**, *786*, 3973. [CrossRef]
64. Giménez, B.N.; Conte, L.O.; Alfano, O.M.; Schenone, A.V. Paracetamol removal by photo-Fenton processes at near-neutral pH using a solar simulator: Optimization by D-optimal experimental design and toxicity evaluation. *J. Photochem. Photobiol. Chem.* **2020**, *397*, 112584. [CrossRef]
65. Nunes, B.; Antunes, S.C.; Santos, J.; Martins, L.; Castro, B.B. Toxic potential of paracetamol to freshwater organisms: A headache to environmental regulators? *Ecotoxicol. Environ. Saf.* **2014**, *107*, 178–185. [CrossRef]
66. Kaiser, K.L.E.; Ribo, J.M. Photobacterium phosphoreum toxicity bioassay. II. Toxicity data compilation. *Toxic. Assess.* **1988**, *3*, 195–237. [CrossRef]
67. Cukurluoglu, S.; Muezzinoglu, A. Assessment of toxicity in waters due to heavy metals derived from atmospheric deposition using Vibrio fischeri. *J. Environ. Sci. Heal. Part A* **2013**, *48*, 57–66. [CrossRef]
68. Peraferrer, C.; Martínez, M.; Poch, J.; Villaescusa, I. Toxicity of Metal–Ethylenediaminetetraacetic Acid Solution as a Function of Chemical Speciation: An Approach for Toxicity Assessment. *Arch. Environ. Contam. Toxicol.* **2012**, *63*, 484–494. [CrossRef]